Production of Thermonuclear Neutrons from Deuterium-Filled Capsule Implosions Driven by *Z*-Pinch Dynamic Hohlraums

C. L. Ruiz,[1] G. W. Cooper,[2] S. A. Slutz,[1] J. E. Bailey,[1] G. A. Chandler,[1] T. J. Nash,[1] T. A. Mehlhorn,[1] R. J. Leeper,[1] D. Fehl,[1] A. J. Nelson,[2] J. Franklin,[3] and L. Ziegler[4]

[1]*Sandia National Laboratories, Albuquerque, New Mexico 87185, USA*
[2]*University of New Mexico, Albuquerque, New Mexico 87131, USA*
[3]*K-Tech Corporation, Albuquerque, New Mexico 87106, USA*
[4]*Bechtel-Nevada, Las Vegas, Nevada 89193, USA*

(Received 12 March 2004; published 29 June 2004)

Evidence for the first production of thermonuclear neutrons by *Z*-pinch dynamic hohlraum driven deuterium-filled capsules is presented. The average neutron energy and yield isotropy measured is consistent with thermonuclear fusion production. The addition of Xe gas to certain capsules suppressed the fusion neutron yields by an order of magnitude, consistent with a thermonuclear production process. The ion temperature deduced from the neutron energy distribution was 4.8 ± 1.5 keV and typical yields were $1–5 \times 10^{10}$.

DOI: 10.1103/PhysRevLett.93.015001 PACS numbers: 52.59.Qy, 52.70.La, 52.70.Nc

Indirect-drive inertial-confinement fusion (ICF) implodes a *dd*- or *dt*-filled capsule by converting energy from a laser beam, ion beam, or *Z*-pinch plasma into x rays that fill a hohlraum, a radiation confinement cavity [1]. The *Z*-pinch dynamic hohlraum (ZPDH) employs a high-atomic-number annular *Z*-pinch plasma that implodes onto a cylindrical low-density CH_2 foam [2–7]. The impact of the *Z*-pinch plasma onto the foam launches a radiating shock wave that propagates inward toward the centrally located capsule. This shock is the main radiation source for heating the hohlraum. The high-opacity *Z*-pinch plasma, behind the shock wave, traps the radiation and serves as the hohlraum wall. The trapped radiation implodes a capsule located at the center of the foam. Efficient x-ray generation makes this process an attractive approach to inertial-confinement fusion [3–7]. Recent dynamic hohlraum research progress [3,6,7] has enabled the first x-ray observations [7,8] of high temperature and density capsule implosion cores driven by ZPDH radiation.

In this Letter, we present evidence for thermonuclear neutrons produced by ZPDH driven implosions of deuterium-filled capsules. To the best of our knowledge, these are the first neutron measurements obtained from capsule implosions driven by a nonlaser laboratory source. The novelty of this approach motivated using several techniques to determine that neutrons were thermonuclear in origin. Such measurements are important because alternative, nonthermonuclear neutron production processes were previously found to exist in *Z*-pinch and dense plasma focus plasmas [9]. Such processes typically involved the creation of directed energetic ions during the plasma disruption, leading to the production of nonthermal, "ion beam" generated *dd* neutrons. If not properly diagnosed, neutrons produced by these nonthermal processes could be misinterpreted as thermonuclear in origin. This Letter focuses on the neutron measurements and the analysis that together led us to deduce a thermonuclear origin for the neutrons observed.

Neutrons produced in a thermonuclear plasma have a fusion energy of 2.45 MeV and isotropic yield. Thus, both neutron energy and yield were measured as a function of angle verifying that the neutrons produced were consistent with a thermonuclear origin. In addition, "null" experiments were conducted in which a small amount (0.6 atm) of xenon gas was added to the standard 10–20 atm deuterium plus 0.085 atm argon capsule gas mixture. Simulations [7] indicate that the xenon radiation losses attenuate the peak capsule temperature and suppress the thermonuclear fusion yield by a factor of 20. The presence of this xenon was not expected to significantly impact ion-beam *dd*-neutron production processes, if indeed these were present. In the experiments reported here, the addition of xenon reduced the neutron yield by a factor of at least 20, strong evidence that the neutrons are thermonuclear.

The experiments reported here used the Sandia National Laboratories 20 MA *Z* facility [2,10] to drive a nested, 10–12 mm high wire array [3,4,10]. The 40-mm diameter outer array was comprised of 240, 7.8-mm diameter tungsten wires, while the inner array at 20-mm diameter was comprised of 120, 7.8-mm diameter tungsten wires. At the center of each array was mounted a 10–12-mm high, 6-mm diameter, 14 mg/cm^3 CH_2 cylindrical foam converter. Centered in the foam converter was a spherical 2-mm-diameter ICF capsule with a (43–80)-mm plastic wall thickness. A numerical study [7] was performed to determine the dimensions of the converter and capsule. These standard capsules were typically filled with 10–20 atm of deuterium gas mixed with 0.085 atm of argon gas. Argon was added as a spectroscopic marker permitting core electron temperature and density

measurements without seriously degrading neutron production [8]. These configurations were not optimized for neutron production but represent compromises resulting from capsule fabrication constraints and diagnostic access requirements.

Our suite of neutron diagnostics consisted of time-resolved and time-integrated detectors. Four plastic scintillation detectors were used in pairs as neutron time-of-flight (NTOF) detectors. Time-integrated indium activation measured the total neutron yield and isotropy. A schematic of the paired detectors for NTOF and indium activation measurements is shown in Fig. 1. The scintillation detectors consisted of 2.54 cm thick by 7.6 cm diameter Bicron BC-418 plastic scintillator coupled via a light guide to fast Hamamatsu R5945 mesh-type phototubes. Two of these ("side-on") detectors A and B were located along a single line-of-sight at 102° with respect to the pinch z axis and at distances of $L_A = 742$ cm and $L_B = 839$ cm, respectively, from the ICF capsule. Another pair of "on-axis" detectors C and D were located on a single line of sight along the z axis at distances of $L_C = 730$ and $L_D = 809$ cm, respectively, below the capsule center. All the detectors were shielded against the hard-x-ray bremsstrahlung background characteristically produced by Z pinches [11]. These shields consist of 20 cm of lead between the source and the detectors and 5 cm of lead at the sides and backs of the detectors. In the case of the side-on detectors, the neutrons exit the Z machine via an evacuated pipe that passes through the water section of Z, which serves as an effective collimator, and minimizes neutron scattering effects. Since the neutrons exiting the bottom of Z do not pass through the water section, an annular polyethylene collimator was introduced in front of the on-axis detectors to similarly reduce neutron scattering effects. The Z machine restricts our measurements to the NTOF distances prescribed above.

The goals of paired detector configurations in the NTOF technique are the absolute determination of the neutron average velocity, $\overline{v}$, and birth time, t_0, for each line of sight. The neutron velocity and birth time are given by $\overline{v} = (L_b - L_a)/(\bar{t}_b - \bar{t}_a)$ and $t_0 = (L_b\bar{t}_a - L_a\bar{t}_b)/(L_b - L_a)$, where a and b are A and B or C and D, respectively. Quantities $\bar{t}_a$ and $\bar{t}_b$ are the neutron arrival times determined from the weighted time averages of the time dependent neutron signals. Inferring the neutron velocity and birth time in this manner is an essential point of this Letter. Another advantage of using paired side-on and paired on-axis NTOF detectors is that the configuration improves our ability to identify ion beams as a contributing source of dd neutrons. Such ion beams, if present, are expected to be axially directed and would result in higher observed neutron energies (>2.45 MeV) in the axial direction. But neutrons from axially directed ions, observed side on (near 102° relative to the z axis), will have an energy consistent with 2.45 MeV. Thus, by measuring neutron energies axially and nearly orthogonally to the pinch z axis, ion-beam contributions to the neutron production are readily identified. Figure 2(a) shows the NTOF signals for one standard capsule (deuterium and argon filled) experiment. The two side-on A and B signals are superimposed. The two corresponding on-axis C and D signals are shown in Fig. 2(b). These measurements were repeated when xenon was added to the fuel mixture with the expectation of suppressing thermonuclear neutron production. The side-on A signal obtained from such a null capsule experiment is shown in superposition with an A signal from a "standard" capsule experiment without xenon in Fig. 2(c). The null capsule produced no discernible neutron signal in any detector at A, B, C, and D positions. Based on the signal to noise quality of the signals, the reduction is at least a factor of 20. Similar results were observed in three separate null capsule experiments. The magnitude of the observed decrease in neutron yield is consistent with the decrease predicted by the simulations [7].

Neutron velocities were measured for all capsule experiments. Based on the method described above, we then

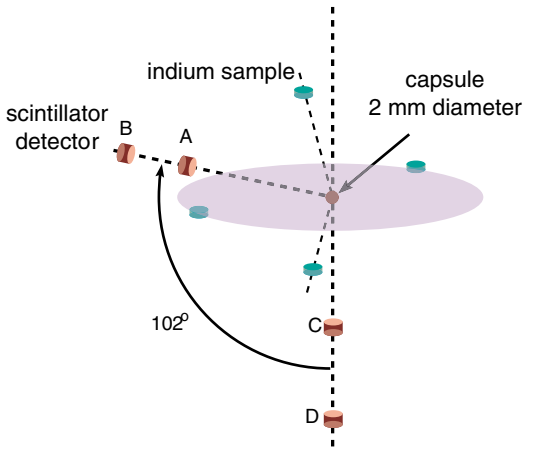

FIG. 1 (color). Schematic diagram of experimental layout. Detectors A, B, C, D, and indium samples not drawn to scale.

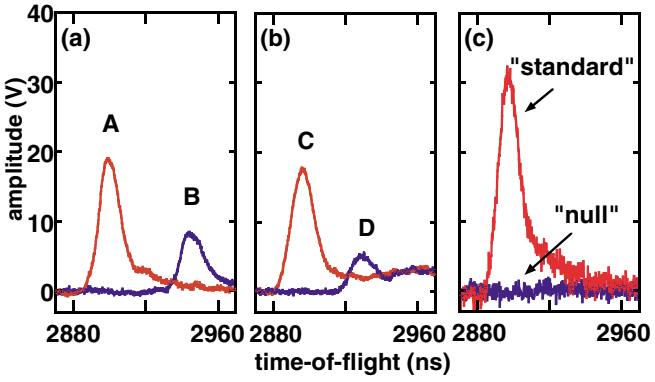

FIG. 2 (color). Representative neutron time-of-flight signals: (a) side-on signals from detectors located at A (742 cm) and B (839 cm); (b) on-axis signals from detectors located at C (730 cm) and D (809 cm) for the same Z shot as shown in (a); (c) side-on signals from the detector located at A (742 cm) for a standard and a null shot.

estimated a separate grand average velocity for the side-on and on-axis measurements. These estimates contain both systematic and statistical uncertainties. The systematic NTOF error is estimated to be approximately 1.2 ns, due to the maximum time that a 2.45 MeV (velocity of 2.17 cm/ns) neutron spends traversing the one-inch thick scintillator. The statistical errors are estimated from the data spread and added in quadrature. Based on these averages, we infer neutron energies from side-on and on-axis detectors to be 2421 ± 110 keV and 2555 ± 120 keV, respectively.

The neutron birth time t_0 can be estimated from both the side-on and the on-axis time centroids $\bar{t}_a$ and $\bar{t}_b$. This time can be compared with time-resolved measurements of x-ray emission from the capsule implosion core obtained with spectroscopic and photoconducting diode instruments [8]. As a reference, we employ the peak in the Z-pinch x-ray power measured by a set of filtered x-ray diodes located to the side of the pinch. The capsule implosion x-ray emission occurs 3–5 ns prior to the side-on Z-pinch x-ray power maximum [8]. The average value of t_0 is -3.0 ± 9.0 ns, i.e., 3 ns before stagnation, in excellent agreement with the capsule implosion x-ray measurements and numerical simulations. The large uncertainty results because t_0 is extrapolated from time-centroid measurements made between two detectors separated by a small distance (example, $L_B - L_A = 97.4$ cm) compared with the large distance of detectors A and B from the neutron source.

The neutron signals shown in Figs. 2(a)–2(c) are consistent with Gaussian-shaped pulses (suggestive of thermonuclear dd fusion) but with skewed tails due to contributions of neutrons scattered from the lead shields surrounding the NTOF detectors. The total time spread Δt_{meas} (FWHM) of each signal is due to separate time spread contributions from neutron time broadening Δt_T of the Maxwellian ion distribution, the detection-time-spread Δt_{sc} for neutrons traversing the scintillator (1.2 ns), the intrinsic time resolution Δt_p of the phototube (3.5 ns), and spread Δt_{scat} from neutron scattering. We believe neutron scattering from 20 cm of Pb had a negligible effect on Δt_{scat} because MCNP (a Monte Carlo neutron-photon transport code) modeling [12] indicated that the time spread at FWHM due to scattering was small when compared to the phototube time spread. All remaining spreads were added in quadrature and subtracted from Δt_{meas} to obtain the neutron time spread Δt_T. This time spread was transformed to a neutron energy width ΔE (keV), which can be related to the ion temperature by using the neutron energy distribution function and ΔE developed by Brysk [13]. By inserting the appropriate $d(d, n)^3$He reaction masses and an average neutron energy of 2450 keV, one finds that the average ion temperature kT is given by $(\Delta E/82.5)^2$, where kT and ΔE are in keV units. The resulting average ion temperature for all standard capsule experiments was estimated to be 4.8 ± 1.5 keV using data from the side-on detectors only, which had the lesser scattering contributions. Since thermonuclear production will be limited by capsule disassembly [1] to less than 1 ns, the time-of-flight spread of the neutron signal at our detector should be dominated by thermal broadening of the neutron energy spectrum and, thus, affords an approximate ion temperature measurement. This average temperature estimate is higher than the 0.8–1.0 keV core electron temperature measurement obtained via argon spectroscopy measurements reported recently [8]. This difference is consistent with computer simulations, which predict ion temperatures of about 5 keV which are substantially above the electron temperature even in the central hot neutron producing region. The electron temperature measured with Ar tracer spectroscopy is substantially lower, since the neutron emission is strongly weighted to the hottest plasma ion temperature while the 3–4 keV Ar x rays are preferentially emitted from plasmas with lower temperatures.

Indium activation was used to estimate total neutron yield and isotropy. This time-integrated diagnostic is based on the reaction $^{115}\text{In}(n, n')\ ^{115m}\text{In}$ and is a standard for measuring dd neutron yields in ICF experiments [14]. A competing $^{115}\text{In}(\gamma, \gamma')\ ^{115m}\text{In}$ reaction [15] must be taken into account due to the hard bremsstrahlung background on Z. The ^{115m}In metastable state emits a 336 keV gamma ray, which we measured with a high-purity germanium detector. Cylindrical (2.5-cm diameter by 1.25-cm thick) indium samples were placed at 15° (near the on-axis direction), on the side at 90° (near the side-on direction), and 165° (nearly opposite the on-axis direction).

Absolute calibration of the neutron yield depends on corrections due to the solid angle subtended by the indium sample, distance of the sample from the capsule, and the neutron scattering and attenuation due to surrounding hardware. These corrections, estimated to be accurate to within a few percent, were calculated using the code MCNP [12] and assumed an isotropic neutron yield into 4π and a 5 keV thermonuclear dd fusion source. We defined the yield for any given shot to be the unweighted average of the yields obtained from each of the samples. Assuming all activation to be produced by neutrons, we find the following results: The grand average neutron yield for the standard capsule shots was $(3.4 \pm 1.1) \times 10^{10}$ while it was only $(3.6 \pm 1.1) \times 10^9$ for the null shots, i.e., capsule shots with xenon present. This decrease in yield of the null capsules by a factor of approximately 9.4 as measured with indium compares with a decrease of more than 20 observed with the time-of-flight detectors. This observed difference may imply that the residual $\sim 3.6 \times 10^9$ yield inferred on the null experiments is in fact due to bremsstrahlung-induced activation of the indium.

Unfortunately, the activation results cannot be corrected accurately for this background due to its observed shot-to-shot variability. One may argue that the bremsstrahlung-induced activity, however, does not

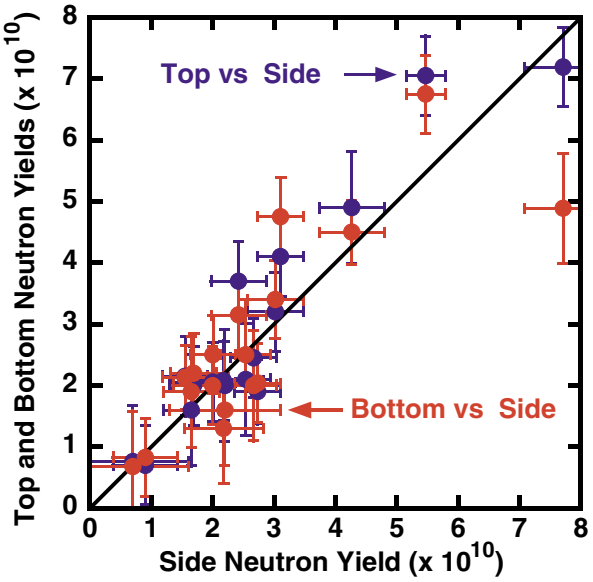

FIG. 3 (color). Neutron fluences measured with the indium activation diagnostic converted to neutron yields. To indicate isotropy, yields obtained on axis (top and bottom) are plotted versus each corresponding side-on yield. A line of slope one is shown only as a guide.

dominate the reported yield from standard capsule experiments for the following reason. The standard capsule shots produce on the average 9.4 times more indium activity than the null shots containing xenon. Since the experimental configurations in these two cases are virtually identical, one would expect that the bremsstrahlung backgrounds would be similar. The induced ^{115m}In activities observed on the null shots, therefore, should be representative of an upper limit for the bremsstrahlung-induced background on the capsule shots. We conclude that the neutron-equivalent background levels due to bremsstrahlung are at most approximately 0.4×10^{10} (or about 10% to 15% of the standard shot yield). Thus, the average standard capsule yield of 3.4×10^{10} is representative of the true neutron yield within the 30% overall uncertainty of the measurement.

The indium detectors also address the issue of yield isotropy. In principle, the integral of the NTOF detector signals also address isotropy; however, adequate neutron response calibrations were not available. Figure 3 plots neutron yields (assumed to be isotropic) as measured on the top and bottom of the Z pinch versus yield measured on the side for all shots. The error bars represent 2σ uncertainties. A line of slope one, which represents an isotropic yield, has been added as a guide only. Although there is some scatter in the data, the yield appears to be isotropic within the uncertainty of the measurement. We note that the maximum observed asymmetry is about 25%, which is of the same order as the estimated bremsstrahlung-induced background. Thus, the observed scatter in the data could be due to random asymmetries in the bremsstrahlung-induced activation, although this cannot be confirmed. We also note that, for pure beam-target interactions, the anisotropy should exceed 50% [16] so these data appear to preclude a pure beam-target mechanism. We conclude that within the uncertainty of the measurement the activation results are consistent with isotropic thermonuclear fusion.

In conclusion, we find the evidence for thermonuclear production in Z dynamic hohlraum experiments is compelling. The neutron energy is the same within errors at two nearly orthogonal directions and is centered at nearly 2.45 MeV. The yield is consistent with isotropy to less than 25%. The yield is suppressed with the addition of a high Z material (Xe) to the capsule deuterium fuel to enhance radiation losses. The neutrons are born 3 ns prior to stagnation. Importantly, the ion temperature inferred from our measurements provides a new tool for evaluating the physics of dynamic hohlraum driven capsule implosions.

We appreciate the interest and support from J. P. Quintenz and M. K. Matzen. This work was performed under the auspices of the U.S. DOE by Sandia National Laboratory under Contract No. DE-AC04-94AL85000.

[1] J. Lindl, Phys. Plasmas **2**, 3933 (1995).
[2] M. K. Matzen, Phys. Plasmas **4**, 1519 (1997); V. P. Smirnov, Plasma Phys. Controlled Fusion **33**, 1697 (1991); J. H. Brownell *et al.*, Phys. Plasmas **5**, 2071 (1998).
[3] T. J. Nash *et al.*, Phys. Plasmas **6**, 2023 (1999).
[4] R. J. Leeper *et al.*, Nucl. Fusion **39**, 1283 (1999).
[5] D. L. Peterson *et al.*, Phys. Plasmas **6**, 2178 (1999); J. Lash *et al.*, in *Proceedings of Inertial Fusion Science and Applications 99, Bordeaux, France, 1999*, edited by C. Labaune, W. J. Hogan, and K. A. Tanaka (Elsevier, Paris, 2000), Vol. I, p. 583; S. A. Slutz *et al.*, Phys. Plasmas **8**, 1673 (2001).
[6] J. E. Bailey *et al.*, Phys. Rev. Lett. **89**, 095004 (2002).
[7] S. A. Slutz *et al.*, Phys. Plasmas **10**, 1875 (2003).
[8] J. E. Bailey *et al.*, Phys. Rev. Lett. **92**, 085002 (2004).
[9] O. A. Anderson *et al.*, Phys. Rev. **110**, 1375 (1958); P. J. Bottoms *et al.*, in *Proceedings of the Plasma Physics and Controlled Nuclear Fusion Research Conference, Novosibirsk, 1968* (IAEA, Vienna, 1969), Vol. 2, p. 67; J. E. Bailey *et al.*, Appl. Phys. Lett. **40**, 460 (1982); W. Stygar *et al.*, Nucl. Fusion **22**, 1161 (1982); V. V. Vikhrev, Sov. J. Plasma Phys. **12**, 262 (1986).
[10] T. W. L. Sanford *et al.*, Phys. Plasmas **9**, 3573 (2002).
[11] M. Derzon *et al.*, Rev. Sci. Instrum. **70**, 566 (1999).
[12] J. S. Hendricks, MCNP4C2, LA-UR-01-858 (2001).
[13] H. Brysk, Plasma Phys. **15**, 611 (1973).
[14] G. W. Cooper and C. L. Ruiz, Rev. Sci. Instrum. **72**, 814 (2001).
[15] J. J. Carroll *et al.*, Phys. Rev. C **43**, 1238 (1991).
[16] H. Liskien and A. Paulsen, Nucl. Data Tables **11**, 569 (1973).